This is the Accepted version of the article; the final Published version of the paper can be accessed in the journal:

Fusion Engineering and Design Volume 121, October 2017, Pages 152-158, ISSN 0920-3796,

https://doi.org/10.1016/j.fusengdes.2017.06.040

Accelerometers data processing for boiling onset detection on the LIPAc Beam Stopper

F. Arranz, P. Olmos, B. Brañas
[a]*CIEMAT. Avda. Complutense 40. 28040 Madrid. Spain.*

ABSTRACT

The LIPAc (Linear IFMIF Prototype Accelerator) is a prototype that ends in a dump made of copper with conical shape and cooled by water moving at high speed on the outer surface.

In case the beam reaches the dump with abnormal misalignment or offset, the local temperatures at the water-copper surface will give rise to boiling onset which can be used as a warning flag before an excessive thermal stress distribution could endanger the mechanical integrity of the Beam Dump.

Previous experiments having the same goal were carried out with hydrophones to detect the onset of boiling [doi:10.1016/j.fusengdes.2015.01.011]. The current article deals with the treatment of the signal coming from an accelerometer.

The article will go into detail of data treatment to refine the detection of the boiling onset, even if noise coming from external or undesired sources is mixed with the boiling signal, which prevents in this case the use of the RMS as a monitoring parameter.

Recommendations are given for the implementation in the cooling system of the LIPAc Beam Dump to be installed in Rokkasho.

Keywords: Boiling; Acoustic; Beam dump; IFMIF; accelerometer; Interlock

1. Introduction

The International Fusion Materials Irradiation Facility, also known as IFMIF, will be a test facility in which candidate materials for the use in fusion reactors can be fully qualified. The LIPAc (Linear IFMIF Prototype Accelerator) is a prototype of one of the two IFMIF accelerators [1]. Its objective is to validate the low energy part (9 MeV) of the IFMIF linacs (40 MeV, 125 mA of D+ beam in continuous wave). It will not have a target and hence a dump is needed to stop the deuteron beam.

The LIPAc BD (Beam Dump) which stops the deuteron beam consists of a cone made of copper, whose inner surface absorbs a power of 1.12 MW, with up to 2.5 MW/m^2 peak power density in nominal conditions. This piece is cooled by water in counter-beam direction at high velocity through an annular channel formed between it and a second piece (shroud or outer cone) [2].

The shape of the beam and the deviations from nominal value, give rise to areas within the inner cone where higher temperatures and thermal stresses may be reached, situations that do compromise the mechanical stability of the whole piece. The pressure has been chosen to have near-saturation conditions, therefore when the temperature in the cone-water interface exceeds a certain threshold boiling occurs and its detection can trigger a safety interlock to stop the beam. So the prompt identification of the boiling onset plays an important role in the alarm subsystem.

This boiling onset can be detected by means of hydrophones introduced in the cooling water, as described in a previous article [3]. Here we explore the suitability of accelerometers to perform this task. These sensors possess some operative advantages: (1) they can be attached to the external surface of the pressure vessel, not requiring penetration of the wall; (2) their high frequency response is less sensitive to common external acoustic noises which become largely damped by the massive structure; (3) their response is essentially independent of where they are placed on the structure; (4) the same sensor can be used to monitor flow induced vibrations (low frequency) and boiling (high frequency); (5) finally, there are a wide range of available models in the market that are radiation hard at the levels expected in the installation. This work describes the signal treatment that is required for the boiling onset detection when the raw signal is mixed with random bursts occurring as a consequence of high speed flows, vortex shedding, cavitation and/or remaining gases in the circuit.

There are key works in fusion components cooling systems where accelerometers are used, such as the Plasma Facing Components analysis carried out for the ITER divertor [4], which demonstrates the suitability of accelerometers signals to detect Critical Heat Flux (CHF) precursors. The whole range of subcooled boiling can be studied with accelerometers [5], in circular channels with and without turbulence promoters. In comparison with such studies, the current work features a more slender geometry prone to vibrations [6] and therefore to the appearance of noise mixed with the boiling signal.

2. Description of the experimental setup

author's email: fernando.arranz@ciemat.es.

2.1 Prototype of the BD

The device on which the tests have been performed is a 1:1 model of the final version to be installed in the Rokkasho facility, which is thoroughly described in [7]. As can be seen in figures 1 and 3, the BD consists of a 2.5 m long inner cone with an aperture of 0.3 m and a wall of 5 mm in most of it, except the 500 mm near the base with 6.5 mm thickness and the zone of the tip with increasing thickness to provide robustness for mechanical support.

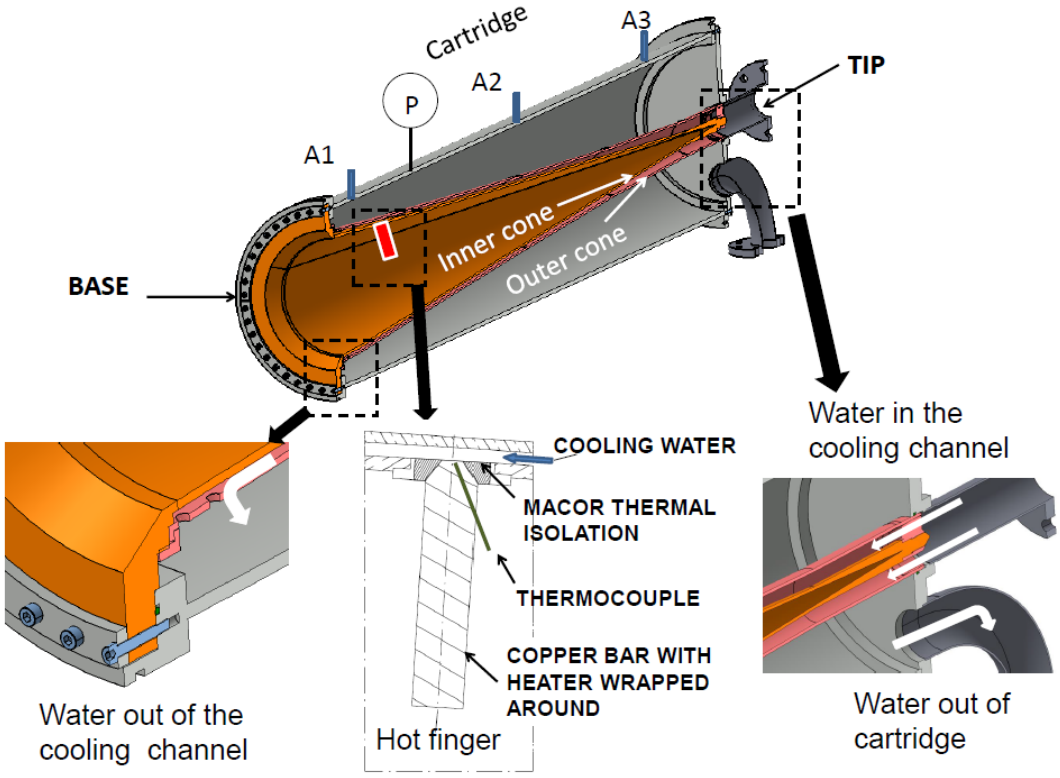

Fig. 1 Cross section of the BD cartridge prototype. A1, A2, A3 are the accelerometer locations.

The cooling channel between the inner cone and the shroud has a varying gap from a maximum of 23 mm near the tip up to a minimum of 5.5 mm at 500 mm from the base of the cone. The outer cone or shroud is actually a succession of truncated cones, so the speed is kept in values that would provide an acceptable heat transfer coefficient to remove the power of the beam with reasonable temperature gradients. With the nominal flow (108 m^3/h), the speed ranges from 9.9 m/s at the tip zone up to 4.3 m/s near the base (Fig. 2).

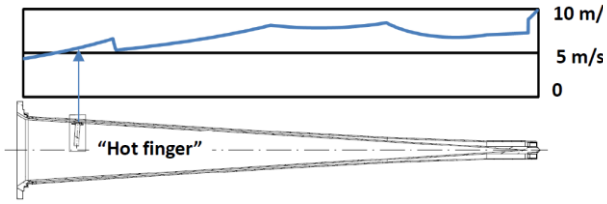

Fig. 2 Water speed profile in the cooling channel (between cones).

The water gets out of the cooling channel in the area of the flange, through holes made on the shroud, and returns backwards to exit the cartridge through the volume defined between the outer cone and the external cylinder (diameter of 0.5 m). The three main components (cones and cylinder) share the same geometric axis, which is placed horizontally.

The cooling water is propelled by a centrifugal pump with a frequency converter to vary the flow rate. The target flow value in nominal conditions is 108 m^3/h, although during the commissioning period smaller flows will be used. In nominal conditions, the water at the inlet of the cartridge is held at a pressure of 3.5 bar (absolute) and a temperature of 31 ºC (defined by the cooling towers on site). Fig. 3 sketches a simplified layout of the hydraulic part of the installation actually used with the prototype to obtain the data used in this article.

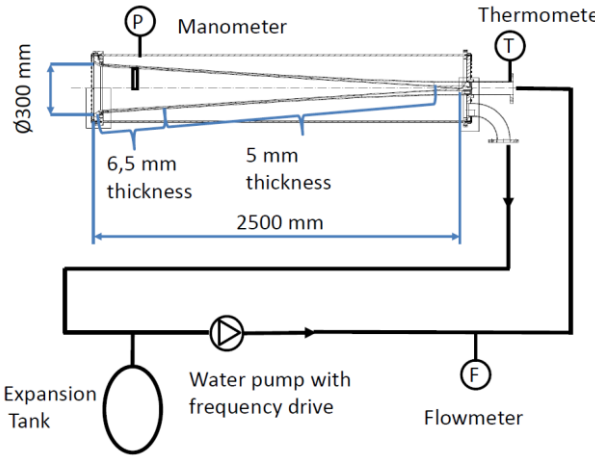

Fig. 3 Simplified sketch of cooling circuit. Thickness of the inner cone wall.

2.2. Localized heating

With the nominal beam, the energy released by the deuterons heats most of the inner cone in an approximately uniform way, and the cooling loop maintains the temperature within safe limits. On the contrary, an abnormal beam profile would produce a dangerous local increase in temperature at the zone where it hits the metal. As a consequence, the inter-cone water in the proximity of this zone can boil and an alarm must be generated. This anomalous situation is the subject of our study.

Since no accelerated particle beam of enough energy and intensity is at hand, the local overheating has been simulated by disposing a "hot finger" that heats a small spot of the inner cone, as indicated in Fig. 1. It has been made of a copper circular rod (1 cm diameter), insulated from the rest of the cone with a ceramic ring (Macor) and from the environment with mineral wool. The copper bar has an electrical resistance wrapped around it. A DC power supply is able to transfer to the water a power density similar to the expected value when the proton beam accidentally deflects, around 250 W/cm^2. The temperature of the rod is monitored with a K-type thermocouple placed at 1 mm from its tip (the part in contact with the water). This thermocouple is also used as the sensing element of the heater controller that switches on/off the power supply to maintain a constant temperature in some of the experiments. The speed of the water at the section of the hot finger is 5.47 m/s with nominal flow. Given the high heat transfer coefficient values with nominal flow, the thermal isolation and the low temperatures involved, only convection is considered through the surface of the hot finger with the water [2].

The experimental set up targets to mimic the conditions of the real operational system, it was not designed to perform fine measurements of heat transfer. Some features worth to mention are: the localized heat spot (1 cm in a 2.5 m long conical shape), the almost horizontal narrow channel (6.15 mm gap where the heater is placed), the highly subcooled fluid (31 ºC bulk temperature) and the turbulent regimens (Re well in excess of 10^5) involved.

2.3. Boiling sensor

The accelerometer, glued with cyanoacrylate to the outer part of the cartridge, is a one-axis sensor that measures the radial vibrations with sensitivity of 100 mV/g (g being the acceleration of gravity) and a bandwidth of 20 kHz; it is the model 4518-003 from Brüel & Kjaer. Its output is digitized in the audio card of a PC with 16 bits of resolution sampled at 48 kHz . The accelerometer output is essentially insensitive to the place where the boiling happened because it detects the vibration of the whole structure which is practically independent of the measuring point, at least for the sizes involved. This has been confirmed by placing the device at the three positions (A1, A2, and A3) indicated in Fig. 1, and obtaining similar results.

3. Boiling at rest

It is interesting to start by looking at the pool boiling process with the circuit closed. To do this, the hot finger was first heated with a constant power density of 150 W/cm^2 until a temperature well over the boiling point is reached, then the power was switched off and the system was left to cool down freely. Values of the temperature and digitized amplitudes from the accelerometer were recorded simultaneously for the entire duration of each cycle. Fig 4 (top) shows the temperature variation of one of these records obtained for an absolute water pressure of 1 bar. The curve starts from a point well below saturation; increases relatively fast until it reaches a maximum where fully developed boiling would be expected (but below the Critical Heat Flux) and decays slowly after the power supply was switched off.

The time domain raw signal obtained from the accelerometer is represented in Fig. 4 (bottom). Although this rapidly variable signal indeed confirms the existence of a net increase in the vibration level, it is still inadequate to constitute a true signature of the boiling phenomenon. The usual way to deal with this type of signals is by means of finding the RMS value of the samples contained in sliding non-overlapping time windows, thus producing a kind of signal envelope [8]. The width of such intervals defines the amount of fluctuations allowed in the final pattern, as shown in Fig. 5 where 0.1 and 1 sec windows have been used to form the boiling response. The excellent signal to noise ratio of the black trace allows finding the onset of nucleate boiling (ONB), which corresponds to a temperature of 105ºC measured by the thermocouple. Essentially similar patterns were obtained for different water absolute pressures, with clearly defined ONB that possess the same excess over saturation (about 5ºC) in all the cases.

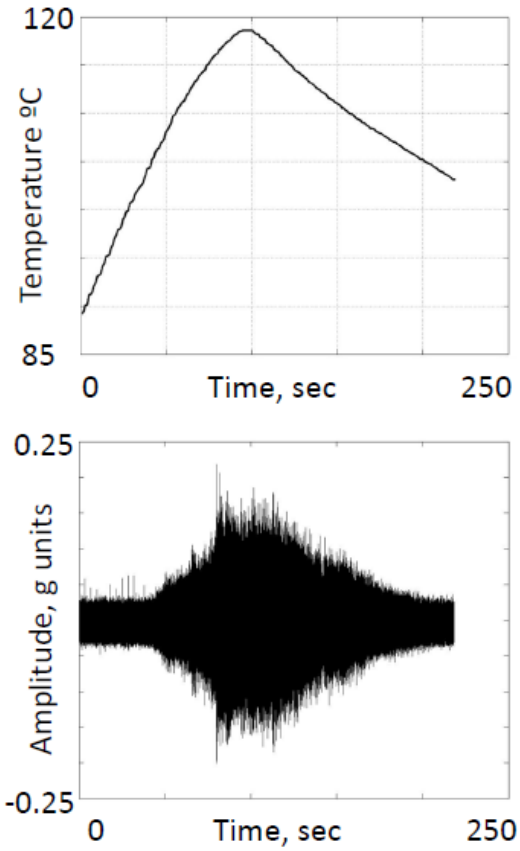

Fig. 4 Evolution of temperature of the hot finger thermocouple during one heating cycle (top). Time domain vibration signal (bottom).

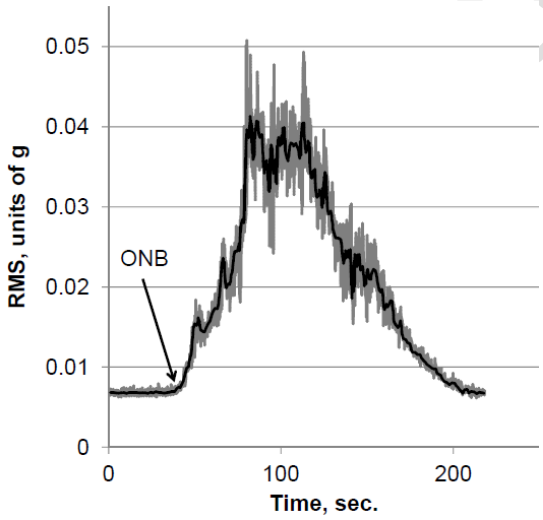

Fig. 5 Pool boiling. RMS signal envelope obtained with two different time windows: 0.1 sec (grey) and 1 sec.(black)

It is possible to give a qualitative explanation of the overall shape of these curves, as follows. Once the nucleation has started, the pressure fluctuations inside the bubbles as they grow up at their sites make the structure vibrate, which explains the initial part of the signal immediately after ONB. When the buoyancy overcomes the surface tension, isolated bubbles begin to detach from these sites and rise (about 10ºC in excess of saturation temperature), coalescing and forming larger voids as the temperature increases and the boiling becomes fully developed. This gives rise to the peaks observed soon after the ONB. During the short path they can travel (6.15 mm of the cooling channel gap) the bubbles go through successive layers of liquid that cool them down rapidly, shrinking their sizes or eventually making them collapse; the fast final rising part of the curve is the consequence of these phenomena. Those bubbles that have survived the action of the cool water, reach the wall of the outer cone (held at the bulk temperature) losing more energy through elastic and inelastic collisions; this is the cause of the peaks found in the upper part of the signal. Once the external power is removed, the system cools down by natural convection, the bubbles give less energy to the cones and finally they disappear dissolved in the water; so the signal decays to the ground level it had before boiling. Note that, in general, the vibrational signatures of two boiling processes carried out in identical conditions differ in their exact shape.

4. Flow without boiling

The highly turbulent flow designed to guarantee good heat dissipation implies that the occurrence of some unwanted phenomenon, known as turbulence noise, becomes highly probable. Under this term we will group different effects, these being for instance air entrainment or dissolution, formation and collapsing of bubbles due to cavitation, vortex shedding and flow induced vibrations [9], all of them coexisting to some extent in an installation like this one. From the practical point of view, the final consequence of all these effects is the increase of the baseline signal magnitude together with the apparition of isolated, randomly distributed, high amplitude bursts superposed to it.

This is seen in Fig. 6 where the flow induced vibrations are depicted for two flow rates: 108 m^3/h (nominal) and 54 m^3/h (grey and black traces respectively); absolute pressure in the circuit was 1.5 bar. A high pass filter (fc=1 kHz) has been applied to get rid of the low frequency noise due to the pumping. Not only is the baseline magnitude sensibly larger in the first case but very loud and intermittent vibrations appear randomly in the form of bursts that are listened like gravel flowing through a metal pipe. They are responsible for the sudden increase in the RMS values of the vibration signals obtained after analyzing records taken at different water flows, the remaining conditions being unaltered (Fig. 7). The slowly growing behavior of the curve at the beginning exhibits a rapidly crescent trend when the flow exceeds 77 m^3/h, thus indicating that there are other contributions to the RMS apart from the otherwise smooth baseline.

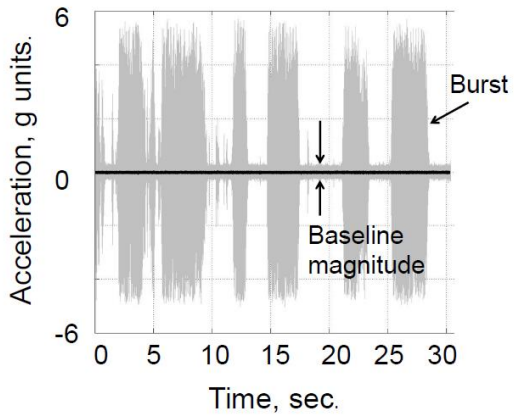

Fig. 6 Flow induced vibrations with frequencies greater than 1 kHz for two water flows: 108 m^3/h (nominal, grey color) and 54 m^3/h (black).

The flow rate at which these bursts begin to show up seems to depend on the temperature and pressure of the water, their repetition rate reducing for higher pressures and lower temperatures. On the contrary, those zones of the signal free from bursts keep their magnitude independently of the pressure, though the fluid temperature has a slight enlargement effect. With the water loop working at its full operating flow rate, the unpredictable pileup of events of high amplitude vibrations becomes an unavoidable fact that we necessarily have to live with. Therefore, the design of the decision algorithm should be able to filter these bursts.

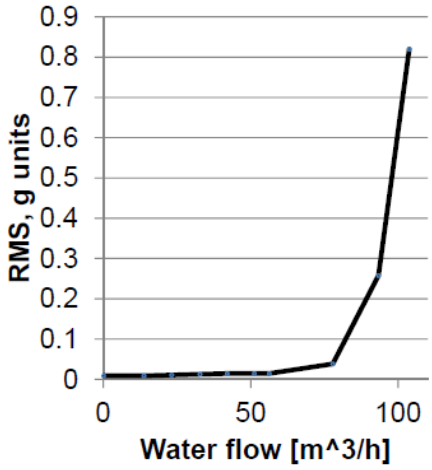

Fig. 7 Variation of the RMS value of 40 sec. vibration records with the water flow; frequencies lower than 1 kHz have been rejected.

5. Flow with boiling.

5.1 Constant temperature conditions.

In this Section the results of experiments of flow boiling at constant temperature will be presented. Using the regulation circuitry, the power supplied to the hot finger was varied in such a way that the temperature measured by the thermocouple was kept constant at a pre-set value. Although this is an unrealistic situation during the operation of the BD, it gives some insight at how the boiling bubbles develop when there is a strong cooling on the surface. Forty seconds of time records were taken after the temperature had stabilized, with the water conditions carefully tuned to minimize the contribution of the (unavoidable) spurious signals.

The first case we consider here was measured at half the nominal flow rate (54 m^3/h), absolute pressure of 1.8 bar at the inter-cone channel (position of hot finger),and the water bulk temperature remained essentially constant (25ºC). The temperature of the hot finger was varied between 100ºC and 190ºC in steps of 5ºC. The raw time signals have been high pass filtered with fc = 1 kHz. No spurious bursts were seen in any of the records. The results of the measured RMS are shown in Fig. 8 (black curve). The ONB suggested by the shape of the plot takes place at around 130ºC while the saturation temperature is 111.6ºC. This gap between ONB and saturation temperature (18.4ºC) is significantly larger than the same gap in the pool boiling experiment (5ºC) and it constitutes a good indication of how the cooling flow removes the power supplied to the heater.

In the same figure 8 (black line), the increment in the RMS magnitude from no boiling value up to the peak in the figure is around 0.1 g, whereas in pool boiling this increment is around 0.03 g (Fig. 5), that could be consequence of the superposition of collapsing events of the bubbles under the dragging flow. Since the lifetime of the bubbles decreases with increasing heat flux and drag velocity [10], the noise source (collapse events) are closer in time and may superpose, thus resulting in an overall magnification of the vibration signal.

The second case considered was measured at the nominal flow rate (108 m^3/h), absolute pressure of 3.5 bar at the inter-cone channel (position of hot finger), and the water bulk temperature being essentially constant 25ºC. The pressure is higher in this case because otherwise the turbulent noise would prevent obtaining any useful information. The temperature of the hot finger was varied between 135ºC and 190ºC in steps of 5ºC. The raw time signals have been high pass filtered with fc = 1 kHz. The results of the RMS are shown in Fig. 8 (grey curve). The ONB cannot be deduced from the shape of the curve because the numerous bursts in the signal are very influential in the RMS value and they appear irregularly (see Fig. 9).

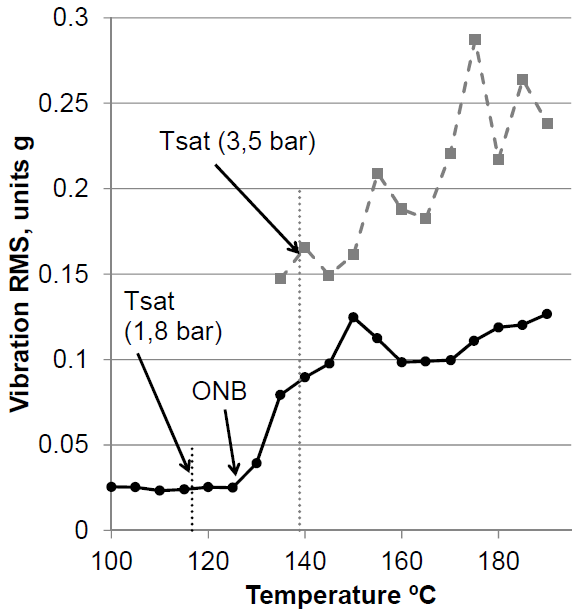

Fig. 8 Evolution of the RMS value of the 40 sec. vibration records with the (controlled) temperature, for a water flow of 54 m^3/s 1.8 bar (black), and for 108 m^3/s 3.5 bar (grey)

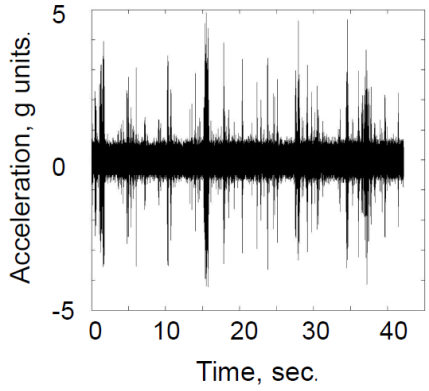

Fig. 9 Example of one time domain record showing boiling and spurious bursts. Flow 108 m3/h.

It was necessary, for the nominal water flow (108 m^3/h), a tool to discriminate the increase in the baseline magnitude of the vibration coming from the boiling, and the discontinuous increase of the signal due to the bursts ,characterized by their high amplitude and irregular appearance.

Figure 10 (top) shows the histogram of amplitudes for a sample taken at 175ºC and therefore with an already developed boiling situation. It can be seen that the tails of the distribution that contain the events corresponding to bursts are of relatively small magnitude. Figure 10 (bottom) shows the histogram of amplitudes for a sample taken without heating, same flow as in the previous case, where it can be seen that the bursts contribution leads to bigger tails.

This suggest that the Full Width Half Maximum (FWHM) of the histograms, rather than the RMS is the parameter to monitor in order to detect the ONB and hence to trigger the alarm.

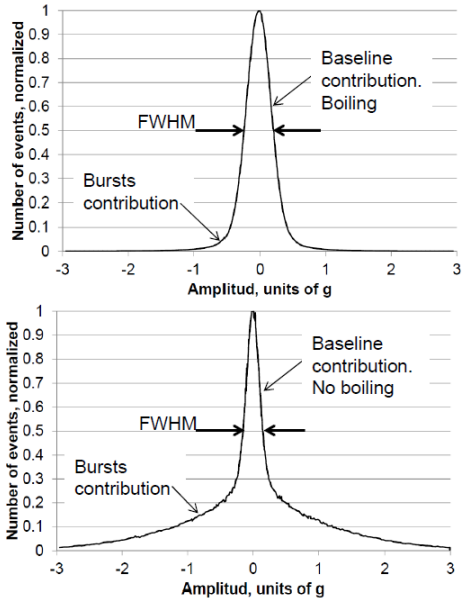

Fig. 10 Histogram of amplitudes of the samples contained in 40 sec. records, with discrete isolated bursts and boiling (top), with long high amplitude bursts an no boiling (bottom)

The values of FWHM computed for nominal flow rate 108 m^3/h, absolute pressure of 3.5 bar at the inter-cone channel (position of hot finger), the water bulk temperature being essentially constant 25ºC, with a high pass filter of fc = 1 kHz are represented as a function of the temperature of the hot finger in Fig. 11 (grey curve). From this curve the ONB can be estimated and a threshold can be set to raise an alarm. As an engineering approach the threshold is set at 10% the total increase of the FWHM value from no boiling up to the highest point where well developed boiling is taking place.

Since some high frequency modes and harmonics of the structure over 1 kHz are excited by so high a fluid velocity, even better SNR can be achieved if an additional higher pass filter (fc=10 kHz) is previously applied to the time domain signals of the same test (Fig. 11, black curve). The ONB is more clearly defined and the alarm threshold with the same criteria than before is closer to the ONB.

Figure 12 shows the spectra analysis of two signal samples with the same conditions except that the grey line corresponds exclusively to the hydraulic noise whereas the black line additionally includes the developed boiling signal. The comparison of the two lines makes it easier to understand why the 10 kHz filter magnifies the effects of the boiling phenomena, for the higher range of

frequencies the contribution of the hydraulic noise decreases with respect to the boiling contribution.

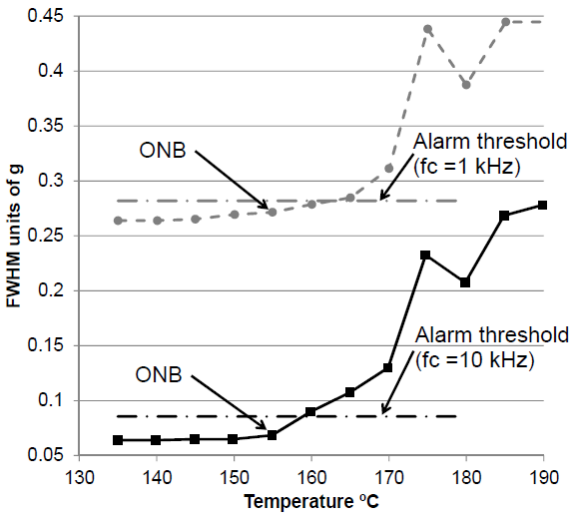

Fig. 11 Evolution of FWHM of the histograms for 40 sec. vibration records with the (controlled) temperature, for a water flow of 108 m^3/h, 1 kHz high pass filter(grey) and 10 kHz high pass filter (black)

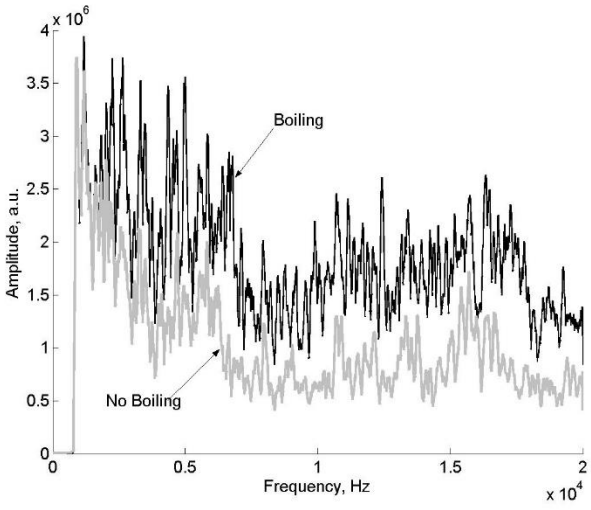

Fig. 12. Spectra analysis for a water flow of 108 m^3/h. Grey line without heat applied. Black line with boiling developed.

5.2 Continuous heating condition.

In real life operation, no temperature control exists and thus we must deal with records evolving in time in a way similar to Fig. 4, but with loud bursts superimposed on them. So the time window approach should be revisited, although in this case, where the method is based on a statistically significant number of samples, some modifications will be necessary. For instance, Fig. 13 (grey curve) shows the result of applying the FWHM method to the samples contained in non-overlapping time windows, 0.1 sec wide, of a record corresponding to a heating cycle. The constant supplied power was 200 W/cm^2 and the temperature reached 180 ºC; the remaining conditions were as before. The bursts have not been filtered and the pattern is not much better than the one obtained with the RMS estimation.

With the same experimental data referred to in the previous paragraph, wider windows were used leading to substantial reductions of these spikes because the high amplitude tails lose their importance as more samples joined the histogram. Fig. 13 (the curve in dashed line) was obtained using increments of 0.1 sec. and overlapping windows including the previous 5 sec. data. From the figure it can be deduced the start of boiling at second 18 with a temperature of 159 ºC at the location of the thermocouple. The threshold to raise the alarm is arbitrarily set at 0.08 g (10% of the amplitude of FWHM recorded values), in order to avoid raising false alarms.

For the data in the current experiment, the maximum delay in the ONB detection is estimated as the time window duration (5 sec.) which translates into an increment of the temperature of about 2.5ºC, something that is acceptable from the engineering point of view in what concerns the safety of the inner cone. The width of the time windows, the time increment for the computation of the FWHM and the threshold for raising an alarm, will be fine-tuned in the final installation of the accelerator´s facility.

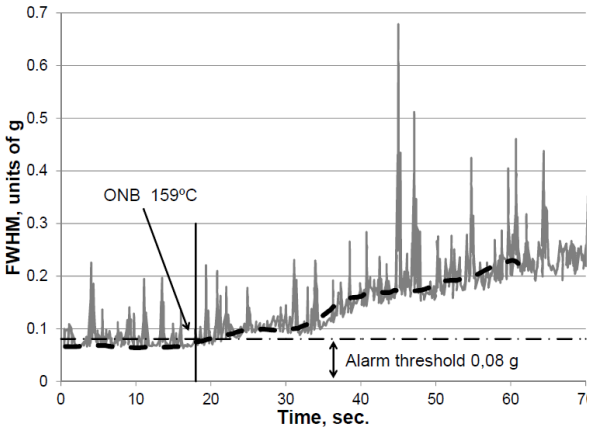

Fig. 13 Time evolution of the envelope vibration signal found by the FWHM method for a heating with boiling experiment at full flow rate (108 m^3/h), using a non-overlapping 0.1 sec time window (grey), and using an overlapping 5 sec. time window with 0.1 sec steps (black discontinuous line)

6. Conclusion

Incipient boiling detection has proven to be an adequate method to detect accidental local overheating on the beam facing wall of the LIPAC´s Beam Dump. This can be done by attaching accelerometers on the external container wall.

In comparison with the use of hydrophones, the accelerometers have the advantages of being non-invasive, have low sensitivity to environmental noises and yield a signal that is independent of the boiling location.

These sensors are particularly useful in those configurations where localized heating takes place in confined horizontal channels because they detect the vibrations that the bubbles induce on the structure, either through pressure fluctuations of the cooling fluid or as a consequence of direct hits on the container walls.

Given the particular geometrical characteristics of the beam dump, highly turbulent flows are involved and therefore the boiling vibrational signals coexist with other spurious bursts resulting from these turbulence phenomena. Some additional processing is required to avoid false alarms derived from these random pulses. It has been found that the measurement of the FWHM of the distribution of samples contained inside a time window constitutes a simple and reliable method to deal with this type of signal.

Overlapping windows can filter the spikes and improve the SNR at the cost of delaying the response of the alarm system. This delay has been found acceptable for the purpose of protection of the inner cone against excessive temperature and thermal stress.

Acknowledgments

This work has been partially funded by the MINECO Ministry under project FIS2013-40860-R and the agreement as published in the Spanish BOE (BOE n14, p. 1988)

The authors appreciate the careful analysis of the anonymous reviewers.

References

[1] D. Gex, P.Y. Beauvais, B. Bra˜nas, P. Bredy, P. Cara, J.M. Carmona, et al., FusionEng. Des. 88 (2013) 2497–2501.

[2] M. Parro, N. Casal, D. Iglesias, F. Arranz, B. Brañas, Fusion Eng. Des. 87 (2012)332.

[3] D. Rapisarda, P. Olmos, B. Brañas, F. Arranz,D. Iglesias, J. Molla. Fusion Eng. Des. 96–97 (2015) 917–921.

[4] X. Courtois, F. Escourbiac, M. Richou, V. Cantone, S. Constansc. Fusion Eng. Des. 88 (2013) 1722–1726

[5] G.P. Celata, G. Dell'Orco , G.P. Gaspari. Fusion Eng. Des. 28 (1995) 44-52

[6] P. Olmos, D. Rapisarda, F. Rueda, F. Arranz, G. Barrera, B. Brañas,A. García, M. Medrano, J. Olalde, L. Maqueda. Fusion Eng. Des. 89 (2014) 2210–2213

[7] F. Arranz, B. Brañas, D. Iglesias, O. Nomen, D. Rapisarda, J. Lapeña, A. Muñoz, B. Szcepaniak, J. Manini, J. Gómez. Fusion Eng. Des. 89 (2014) 2199–2203

[8] Geraldo I.C., Bose T., Pekpe K.M., Cassar J.P., Mohanty A.R., and Paumel K. Nuclear Eng. Des. 278 (2014) 573–585

[9] Kaneko S., Nakamura T., Inada F., Kato M., Ishihara K., Nishihara T., Mureithi N.W. , Langthjem M.A. (Editors), 2014. Flow-Induced Vibrations: Classifications and Lessons from Practical Experiences. Academic Press. 2nd Edition

[10] Prodanovic V, Fraser D., Salcudean, M. International Journal of Multiphase Flow 28 (2002) 1-19